Integrated High-Resolution Optical Spectrum Analyzer With Broad Operational Bandwidth

Arijit Misra, *Graduate Student Member, IEEE*, Stefan Preußler, Dvir Munk, Moshe Katzman, *Member, IEEE*, Linjie Zhou, *Member, IEEE*, Avi Zadok, and Thomas Schneider

***Abstract*— Precise optical spectrum analysis with high resolution by an economical and reliable device is of much interest in optical science and technology. In this work, we propose a silicon-photonic integrated optical spectrum analyzer comprised of two cascaded filters. A first ring resonator stage selects multiple ultra-narrow spectral bands of equal spacing. The set of bands may be scanned across the spectrum of interest through thermal tuning. A second filter stage separates the multiple sampled bands into different output ports. The free spectral ranges of the two stages are matched. The spectrum is reconstructed using simple, low bandwidth photodiodes. In a proof of concept experiment, the proposed integrated optical spectrum analyzer shows a wide operational range with 128 MHz resolution.**

***Index Terms*— Silicon photonics, ring resonators, optical spectrum analyzer, photonic integrated circuits, optical communication, optical filter.**

I. Introduction

HIGH-PRECISION analysis of the power spectral density is among the most fundamental measurement protocols. It is applied in a wide variety of fields in optics and photonics: spectroscopy of chemical compositions and biological molecules, analysis of band structure in semiconductors [1], sensor readouts, and monitoring of communication networks [2]. The proper function of wavelength division multiplexed (WDM) networks critically depends on tight spectral control and careful monitoring of signal-to-noise ratios, side-mode suppression and more [2]. High-resolution, continuous spectral analysis helps to identify and mitigate detrimental effects such as chromatic dispersion, Kerr nonlinearity, and crosstalk.

Most optical spectrum analyzers (OSAs) are based on motorized rotation of diffraction gratings [3]. These gratings resolve the spectral components of an incident optical signal in different directions. The acquisition duration is restricted by mechanical motion, which may also affect long-term reliability. State of the art commercial instruments reach around 2 GHz resolution at telecommunication wavelengths, however high-resolution grating spectrometers are often expensive, bulky, and complex because of the inverse relationship between spectral resolution and free-space optical path length. Additionally, they are sensitive to environmental shocks and vibrations, which limit their application areas. Interferometer based OSAs provide higher resolution than grating based ones [3]. On the other hand, their spectral ranges are typically narrower, and they also suffer from drawbacks associated with moving mirrors. Heterodyne detection down-converts the optical spectrum to the microwave domain through beating with a fixed frequency optical local oscillator [4]. However, the spectral range is restricted to tens of GHz at most by the bandwidths of detectors and electrical spectrum analyzers. The spectral range may be extended by sweeping the local oscillator frequency [5]. Both methods show a high resolution in the range of ∼20 MHz and are capable of measuring the phase and the amplitude simultaneously. But, they require additional tunable lasers and expensive electronics.

Over the last decade, the nonlinear effect of stimulated Brillouin scattering gained a lot of attention for optical spectrum analysis [6], [7]. Thereby, the narrow Brillouin gain is shifted through the unknown spectrum, amplifies the signal under test and the power is recorded versus the wavelength. These systems show a resolution of 10 MHz, which can be decreased down to 3.4 MHz [8], [9]. The out-of-band rejection and dynamic range of Brillouin-based OSAs were enhanced using polarization pulling [10]. Finally, the combination of Brillouin analysis and heterodyne detection has led to kHz-scale resolutions [11]. The measurement systems are rather complex, as they require a long optical fiber as a Brillouin gain medium, amplifiers, stable and tunable lasers, and high-bandwidth modulators [11].

In many fields of applications, more sturdy and compact devices for optical spectral analysis would be preferable. Photonic integrated circuits might dramatically reduce the size, weight, and cost of OSAs. Within the last years,

Manuscript received June 15, 2020; revised July 14, 2020; accepted July 20, 2020. Date of publication July 23, 2020; date of current version August 3, 2020. This work was supported in part by the Deutsche Forschungsgemeinschaft (DFG, German Research Foundation) under Grant SCHN 716/15-2, Grant SCHN 716/20-1, Grant SCHN 716/21-1, SCHN 716/22-1, and Grant SCHN 716/23-1, in part by the Israel Science Foundation under Grant 1665/14, and in part by the Israel Innovation Authority through PETA CLOUD Consortium, MAGNET Program. *(Corresponding author: Arijit Misra.)*

Arijit Misra, Stefan Preußler, and Thomas Schneider are with the THz Photonics Group, Technische Universität Braunschweig, 38106 Braunschweig, Germany (e-mail: arijit.misra@ihf.tu-bs.de; stefan.preussler@ihf.tu-bs.de; thomas.schneider@ihf.tu-bs.de).

Dvir Munk, Moshe Katzman, and Avi Zadok are with the Faculty of Engineering and Institute for Nano-Technology and Advanced Materials, Bar-Ilan University, Ramat Gan 5290002, Israel (e-mail: avinoam.zadok@biu.ac.il).

Linjie Zhou is with the State Key Laboratory of Advanced Optical Communication Systems and Networks, Shanghai Jiao Tong University, Shanghai 200240, China (e-mail: ljzhou@sjtu.edu.cn).

Color versions of one or more of the figures in this letter are available online at http://ieeexplore.ieee.org.

Digital Object Identifier 10.1109/LPT.2020.3011609

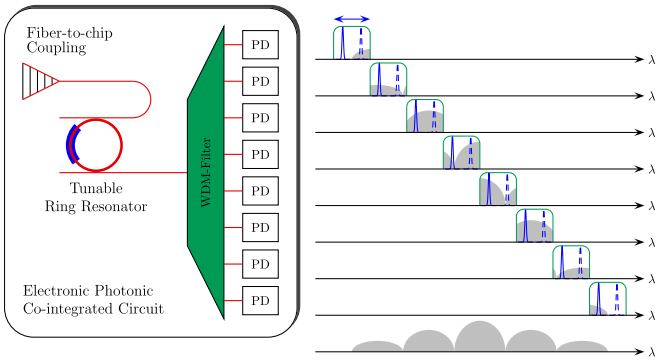

Fig. 1. Schematic illustration of the principle of operation of the integrated optical spectrum analyzer. The blue peaks represent the resonances of the ring, and the green curves denote the filter shape and outputs of the WDM filter. The gray color regions within the WDM filter shapes indicate sliced spectra and the combined spectrum can be seen on the bottom.

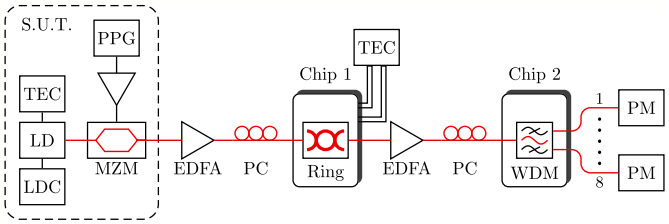

Fig. 2. Setup of the proof of concept experiment for the integrated optical spectrum analyzer consisting of two separate chips. LD: laser diode, TEC: temperature controller, LDC: current source, PPG: pulse pattern generator, MZM: Mach-Zehnder modulator, EDFA: erbium doped fiber amplifier, PC: polarization controller, PM: power meter, SUT: signal under test.

several approaches for integrated spectrum analyzers for different kind of application areas have been proposed and demonstrated [12]–[15]. Most make use of arrayed waveguide gratings (AWGs) in order to separate different spectral components. Integration of AWGs with a large channel count and high spectral resolution, presents a considerable challenge. On chip Fourier transform spectrometers on the other hand generally require complex electronic processing [16].

In this work, we propose an silicon-photonic integrated optical spectrum analyzer that can be realized on a single electronic and photonic co-integrated platform, requires low power, is compact and robust, and supports fast scanning through parallel channels. The performance of the integrated OSA is scalable to broader spectral ranges with high resolution. In a proof of concept experiment, the optical power spectrum of a 20 Gbps pseudo-random bit sequence (PRBS) signal, is characterized over 50 GHz bandwidth with a spectral resolution of 128 MHz ($\sim$ 1 pm).

II. Operation Principle

The concept of the proposed photonic-integrated OSA is illustrated in Fig. 1. It comprises of two cascaded filter stages. The first stage is a ring resonator with high Q-factor, which is characterized by discrete and narrow transmission resonances with uniform free spectral range (FSR) separation. The spectrum of the input signal is therefore sampled at the drop port of the resonator at fixed frequency intervals. The resonance frequencies may be scanned precisely by heating the resonator. The second filter stage is a wavelength-division de-multiplexer device, which separates the spectral samples to different output ports. Each output is collected by a low-bandwidth photodetector. The entire spectrum of the signal is reconstructed by combining power spectra across all output channels. The spectral resolution of the dual-stage OSA is determined by the resonator linewidth, whereas the spectral range equals the combined bandwidths of all wavelength-division channels. The parallel detection of multiple channels helps in reducing the acquisition time. In the application below, the channel spacing of the wavelength division de-multiplexer device was chosen to match the FSR of the ring resonator. In principle, the response of a smaller resonator with a wider FSR may be tuned across several WDM channels. Note, however, that a smaller ring resonator might degrade the Q-factor [17]. In addition, the tuning of the resonator across a broader FSR may require a longer measurement duration.

Silicon is the most suitable material platform for the realization of the proposed integrated OSA [17]. The fabrication processes of silicon-photonic devices are compatible with CMOS electronics. Ring resonators in silicon reach high Q factors, take up comparatively small footprint, and support thermo-optic tuning through the injection of current in metal or highly doped silicon micro-heaters [18]–[21]. The change in the effective index of the guided mode, and the offset in resonance frequencies, are proportional to local temperature change [16], [21]. WDM devices are readily implemented in silicon as well [15], [22]–[27], in the forms of AWGs [15], [23], cascaded Mach-Zehnder interferometers (MZIs) [25], and more complex layout that combine MZIs and resonators [27].

III. Experiment and Results

The setup of a proof of concept experiment is illustrated in Fig. 2. The two filter stages of the proposed OSA were realized on separate devices, connected by optical fiber interfaces. However, such separation is not a fundamental requirement. The optical source was a conventional distributed feedback laser diode, driven by a current source, and regulated in temperature by a controller. The laser light was modulated in a LiNbO3 electro-optic Mach-Zehnder modulator of 40 GHz bandwidth. The modulator was driven by a periodic $2^7 - 1$ bits long binary sequence (PRBS-7) from a pulse pattern generator (PPG). The radio-frequency power of the modulating waveform was 20 dBm. The optical power spectrum of the modulated optical carrier consists of discrete tones with 157 MHz separation. The signal was amplified to 16 dBm by an erbium-doped fiber amplifier (EDFA), and edge-coupled into the ring resonator filter device using lensed fibers. A polarization controller (PC) was used to adjust the state of polarization of the signal at the device input.

The ring resonator used in the proof of concept experiment had an FSR of 18.7 GHz. It was realized on a silicon nitride platform. The device was fabricated in the commercial facility LIGENTEC. Waveguides were 1.8 μm wide and 800 nm high, etched at 82° angle. The racetrack resonator layout included 3.46 mm long straight sections, with bending radius of 100 μm.

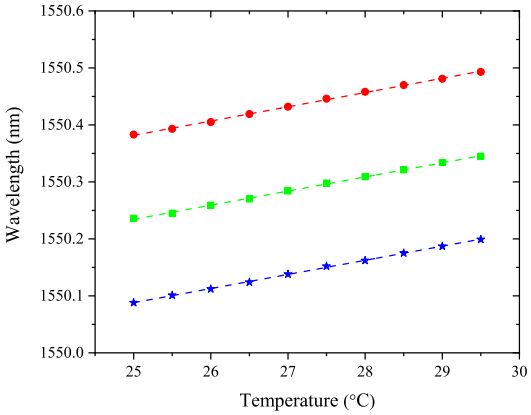

Fig. 3. Measured wavelength shifts of three adjacent ring resonances (red, green, and blue) as functions of temperature. The resonances are red-shifted as temperature increases.

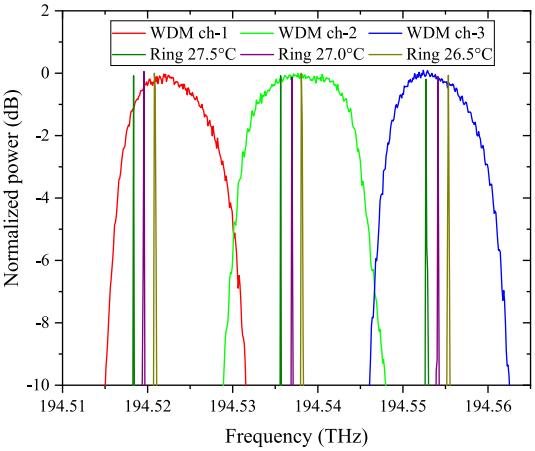

Fig. 4. Measured transfer functions of three adjacent resonances of the microring resonator, taken at three temperatures (see legend for colors), and transfer functions of three adjacent output ports of the wavelength division de-multiplexer device used for optical spectral analysis (see legend for colors).

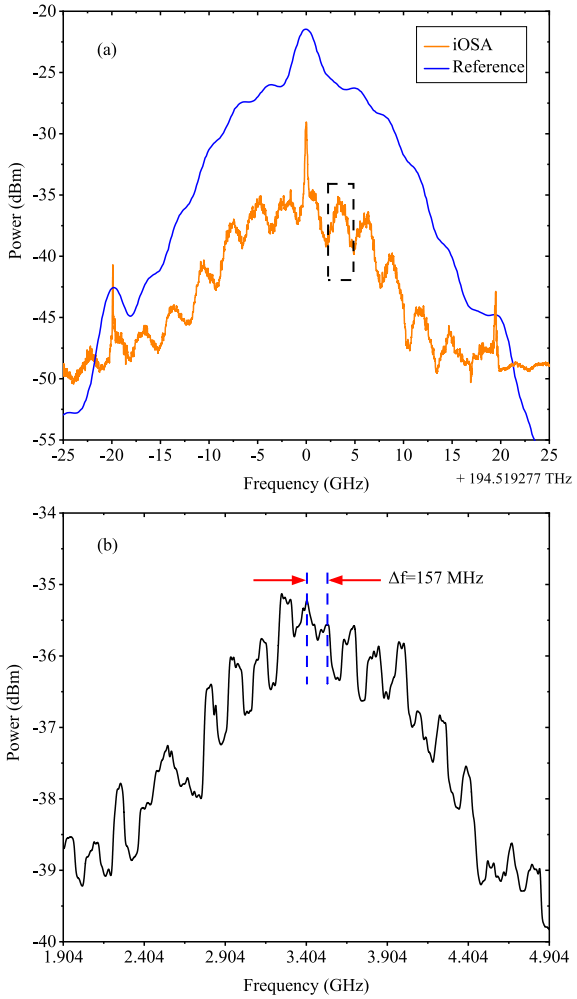

Fig. 5. (a) Measurement results for the proposed integrated optical spectrum analyzer (yellow) in comparison to a grating based one (blue). (b) Magnified view of the measured spectrum, revealing spectral components spaced at 157 MHZ apart. This corresponds to the 20 Gbps non return to zero PRBS-7 signal used as the signal to be analyzed.

The bus waveguide was coupled to the resonator through a directional coupler with 400 nm separation between bus and ring. The coupler layout included S-shaped bends with radii of 100 μm as well. The linewidth of the drop-port periodic resonance transmission bands was 128 MHz (Q-factor of 1.5×10^6 [28]). Thermal tuning was performed by heating the entire chip. The thermo-optic response of the resonance transmission frequencies was $\sim$3 GHz per 1°C. The device stage temperature was regulated by a Peltier element in combination with a temperature sensor. The thermal tuning characteristics of three consecutive resonances is presented in Fig. 3. If the two filter stages are integrated on a single chip, thermal crosstalk may lead to small-scale offsets in the WDM transfer functions while scanning the resonator response. However, thermal crosstalk may be effectively mitigated [21]. Light at the output port of the resonator filter device was amplified by a second EDFA to 16 dBm power, to compensate for coupling losses. A second PC was used to align the state of polarization at the input of the second filter device. The eight-channel, dense wavelength-division de-multiplexer device separated the spectrum of incident light into eight output ports. The de-multiplexer layout consisted of seven cascaded Mach-Zehnder interferometer stages, with ring resonators nested in the shorter arm of each interferometer [27]. The transfer functions of the device are characterized by uniform passbands, strong out-of-band rejection, and sharp spectral transitions between pass and stop bands [27]. Proper function of the device relies critically on the accurate control over phase delays in 14 individual waveguide paths, with 0.01 radians precision [27]. Phase trimming was achieved using local illumination of an upper cladding layer of photo-sensitive chalcogenide glass [27]. The frequency spacing between adjacent channels was 17 GHz, in close agreement with the FSR of the resonator filter stage (see Fig. 4).

The optical power spectrum of the data-carrying signal was characterized by scanning the resonance frequencies of the first filter stage over 17 GHz range with a temperature tuning step of 0.01°C and recording the optical power at three adjacent outputs of the second filter stage. Residual temperature dependence of power transfer through the resonator and non-uniformity of the de-multiplexer passbands were pre-calibrated. Due to the slight mismatch between the FSRs of the two stages (see Fig. 4), data at the three

output ports were collected in series, using successive, separate scans. Sequential operation would not be necessary with better alignment of FSRs in future realizations. The reconstructed signal spectrum is shown in Fig. 5(a), alongside the measurement using a grating based OSA with 4 GHz resolution. As can be seen, finer spectral details are resolved using the silicon-photonic integrated OSA. Fig. 5(b) shows a magnified view of the reconstructed spectrum. The expected periodicity of 157 MHz in the spectrum of the 20 Gbps, PRBS-7 signal can be clearly identified. This spectral period approaches the expected 128 MHz resolution of the microring resonator filter.

IV. Conclusion

In conclusion, we have proposed a concept for a high-resolution integrated-photonic OSA comprised of two consecutive filter devices: a tunable ring resonator and a WDM de-multiplexer of matched FSRs. The proposed device is compact, robust, and can be realized on a single electronic and photonic co-integrated platform with low power consumption. The device would be suitable for measurements at fast acquisition speed over a broad spectral range under challenging environmental conditions. A first proof of concept experiment showed spectral measurements with 128 MHz resolution.

References

[1] N. Tkachenko, *Optical Spectroscopy*. Amsterdam, The Netherlands: Elsevier, 2006.

[2] G. Keiser, *Optical Fiber Communications*. New York, NY, USA: McGraw-Hill, 2000.

[3] D. Derickson, *Fiber Optic Test and Measurement*. Upper Saddle River, NJ, USA: Prentice-Hall, 1998.

[4] D. M. Baney, B. Szafraniec, and A. Motamedi, "Coherent optical spectrum analyzer," *IEEE Photon. Technol. Lett.*, vol. 14, no. 3, pp. 355–357, Mar. 2002.

[5] B. Szafraniec *et al.*, "Swept coherent optical spectrum analysis," *IEEE Trans. Instrum. Meas.*, vol. 53, no. 1, pp. 203–215, Feb. 2004.

[6] T. Schneider, "Wavelength and line width measurement of optical sources with femtometre resolution," *Electron. Lett.*, vol. 41, no. 22, pp. 1234–1235, Oct. 2005.

[7] S. Preussler, A. Wiatrek, K. Jamshidi, and T. Schneider, "Ultrahigh-resolution spectroscopy based on the bandwidth reduction of stimulated Brillouin scattering," *IEEE Photon. Technol. Lett.*, vol. 23, no. 16, pp. 1118–1120, Aug. 2011.

[8] S. Preußler, A. Wiatrek, K. Jamshidi, and T. Schneider, "Brillouin scattering gain bandwidth reduction down to 3.4MHz," *Opt. Express*, vol. 19, no. 9, pp. 8565–8570, 2011.

[9] S. Preußler and T. Schneider, "Bandwidth reduction in a multistage Brillouin system," *Opt. Lett.*, vol. 37, no. 19, pp. 4122–4124, 2012.

[10] S. Preussler, A. Zadok, A. Wiatrek, M. Tur, and T. Schneider, "Enhancement of spectral resolution and optical rejection ratio of Brillouin optical spectral analysis using polarization pulling," *Opt. Express*, vol. 20, no. 13, pp. 14734–14745, Jun. 2012.

[11] S. Preussler and T. Schneider, "Attometer resolution spectral analysis based on polarization pulling assisted Brillouin scattering merged with heterodyne detection," *Opt. Express*, vol. 23, no. 20, pp. 26879–26887, 2015.

[12] E. Ryckeboer *et al.*, "Silicon-on-insulator spectrometers with integrated GaInAsSb photodiodes for wide-band spectroscopy from 1510 to 2300 nm," *Opt. Express*, vol. 21, no. 5, pp. 6101–6108, 2013.

[13] A. Z. Subramanian *et al.*, "Silicon and silicon nitride photonic circuits for spectroscopic sensing on-a-chip," *Photon. Res.*, vol. 3, no. 5, pp. B47–B59, 2015.

[14] G. Micó, B. Gargallo, D. Pastor, and P. Muñoz, "Integrated optic sensing spectrometer: Concept and design," *Sensors*, vol. 19, no. 5, p. 1018, Feb. 2019.

[15] P. Cheben *et al.*, "A high-resolution silicon-on-insulator arrayed waveguide grating microspectrometer with sub-micrometer aperture waveguides," *Opt. Express*, vol. 15, no. 5, pp. 2299–2306, Mar. 2007.

[16] M. C. M. M. Souza, A. Grieco, N. C. Frateschi, and Y. Fainman, "Fourier transform spectrometer on silicon with thermo-optic non-linearity and dispersion correction," *Nature Commun.*, vol. 9, no. 1, p. 665, Dec. 2018.

[17] W. Bogaerts *et al.*, "Silicon microring resonators," *Laser Photon. Rev.*, vol. 6, no. 1, pp. 47–73, Jan. 2012.

[18] H. Qiu *et al.*, "A continuously tunable sub-gigahertz microwave photonic bandpass filter based on an ultra-high-Q silicon microring resonator," *J. Lightw. Technol.*, vol. 36, no. 19, pp. 4312–4318, Oct. 1, 2018.

[19] J. E. Cunningham *et al.*, "Highly-efficient thermally-tuned resonant optical filters," *Opt. Express*, vol. 18, no. 18, pp. 19055–19063, 2010.

[20] D. Geuzebroek, E. Klein, H. Kelderman, and A. Driessen, "Wavelength tuning and switching of a thermo-optic micro ring resonator," in *Proc. 11th Eur. Conf. Integr. Opt. (ECIO)*, pp. 395–398, 2003.

[21] M. Jacques, A. Samani, E. El-Fiky, D. Patel, Z. Xing, and D. V. Plant, "Optimization of thermo-optic phase-shifter design and mitigation of thermal crosstalk on the SOI platform," *Opt. Express*, vol. 27, no. 8, pp. 10456–10471, 2019.

[22] D. Dai, "Silicon nanophotonic integrated devices for on-chip multiplexing and switching," *J. Lightw. Technol.*, vol. 35, no. 4, pp. 572–587, Feb. 15, 2017.

[23] N. Goldstein, L. Pascar, D. Sinefeld, O. Golani, and D. M. Marom, "Fine resolution spectral filtering using a 25 GHz free-spectral range arrayed waveguide grating," in *Proc. Opt. Fiber Commun. Conf.* Optical Society of America, 2015, p. Tu3A.4. [Online]. Available: http://www.osapublishing.org/abstract.cfm?URI=OFC-2015-Tu3A.4, doi: 10.1364/OFC.2015.Tu3A.4.

[24] W. Bogaerts *et al.*, "Silicon-on-insulator spectral filters fabricated with CMOS technology," *IEEE J. Sel. Topics Quantum Electron.*, vol. 16, no. 1, pp. 33–44, 1st Quart., 2010.

[25] F. Horst, W. M. J. Green, S. Assefa, S. M. Shank, Y. A. Vlasov, and B. Offrein, "Cascaded Mach-Zehnder wavelength filters in silicon photonics for low loss and flat pass-band WDM (de-)multiplexing," *Opt. Express*, vol. 21, no. 10, pp. 11652–11658, May 2013.

[26] P. Chen, S. Chen, X. Guan, Y. Shi, and D. Dai, "High-order microring resonators with bent couplers for a box-like filter response," *Opt. Lett.*, vol. 39, pp. 6304–6307, Oct. 2014.

[27] D. Munk *et al.*, "Eight-channel silicon-photonic wavelength division multiplexer with 17 GHz spacing," *IEEE J. Sel. Topics Quantum Electron.*, vol. 25, no. 5, pp. 1–10, Sep. 2019.

[28] A. Misra, S. Preußler, L. Zhou, and T. Schneider, "Nonlinearity- and dispersion-less integrated optical time magnifier based on a high-Q SiN microring resonator," *Sci. Rep.*, vol. 9, no. 1, p. 14277, Dec. 2019.